

Search for production of a Higgs boson and a single top quark in $\mu\mu$ final states in proton collisions at $\sqrt{s} = 13$ TeV

Departamento de Investigacion en Física
Maestría en Ciencias (Física)
Hiram Ernesto Damián

Universidad de Sonora

May 3, 2019



Contenido

- 1 Overview and motivation
- 2 Higgs theory
- 3 tH mechanisms
- 4 Production cross section
- 5 Higgs Branching ratios
- 6 Previous results
- 7 Fitting
- 8 Results
- 9 References
- 10 Supportive slides

Overview

- Through this project we will investigate the production of Higgs boson in association with a single top quark (tH) in proton-proton collisions with the CMS experiment of the LHC. This mechanism of production of the Higgs boson has not been observed before by any experiment.
- Understanding the production of the Higgs boson, as well as its decays are an important part of the physical program of the CERN international laboratory experiments that try to complete the tests to verify the Standard Model, the theory of the fundamental particles



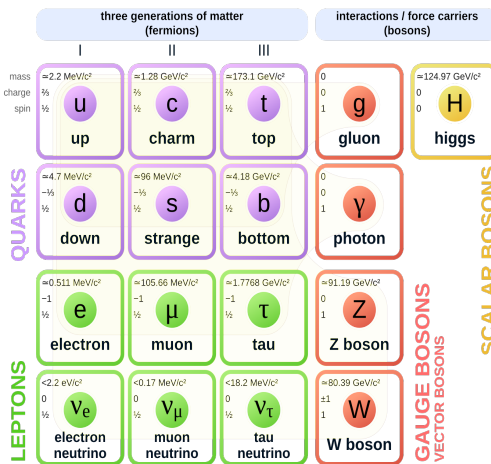
Motivation for single top Higgs (tH)

- Coupling measurement is essential to establish the nature of the Higgs
 - The exploration of Higgs production on the tH channel is subject relatively new. Measurements of CMS and ATLAS are compatible with SM predictions.
 - The tH study explores the relative sign of top-Higgs and W-Higgs couplings.
Small deviations from SM predictions could be associated with physics beyond the standard model (BSM) such as String Theory and Supersymmetry.



Standard Model

Standard Model of Elementary Particles



Electroweak SM Lagrangian

The standard model is a theory of fields with spins 0, $\frac{1}{2}$ and 1. The SM lagrangian

$$\mathcal{L} = \mathcal{L}_{\text{gauge}} + \mathcal{L}_f + \mathcal{L}_{\text{higgs}} + \mathcal{L}_{\text{yukawa}}$$

donde

- $\mathcal{L}_{\text{gauge}} = -\frac{1}{4} [F^{\mu\nu} F_{\mu\nu}] - \frac{1}{4} [G^{i\mu\nu} G^i_{\mu\nu}]$
 - $F^{\mu\nu} = \partial_\mu B_\nu - \partial_\nu B_\mu$
 - $G^{i\mu\nu} = \partial_\mu W_\nu^i - \partial_\nu W_\mu^i - g \epsilon^{ijk} W_\mu^j W_\nu^k$
 - $\mathcal{L}_f = i\bar{\Psi}_L \not{D} \Psi_L + i\bar{\psi}_R \not{D} \psi_R$ is the kinematic term for fermions
 - $D_\mu \Psi_L = (\partial_\mu + igW_\mu + ig'Y_L B_\mu) \Psi_L$
 - $D_\mu \psi_R = (\partial_\mu u + ig'Y_R B_\mu) \psi_R$
 - g and g' are boson coupling constants. ¹

¹L(R) refers to Left and right fields. Y is the weak hypercharge, $Y = T^3 - Q$. Q is charge of particle field and T is weak isospin. $T^3 = \pm 1/2$ for left handed doublets and $T^3 = 0$ for right handed singlets. ▶◀☰≡🔍 6/77



Electroweak SM Lagrangian

Higgs lagrangian

$$\mathcal{L}_{\text{Higgs}} = (D_\mu \Phi)^\dagger (D^\mu \Phi) - V(\Phi^\dagger \Phi) \quad (1)$$

with

- $D_\mu \Phi = \left(\partial_\mu + (ig/2)\sigma^i W_\mu^i - i\frac{1}{2}g' B_\mu \right) \Phi$
 - $V(\Phi^\dagger \Phi) = -\mu^2 \Phi^\dagger \Phi + \frac{1}{2}\lambda(\Phi^\dagger \Phi)^2, \quad \mu^2 > 0$
 - $\Phi = \begin{pmatrix} \phi^+ \\ \phi^0 \end{pmatrix}$ is a SU(2) doublet.
 - σ^i are the Pauli matrices.
 - Φ is higgs field which is a complex scalar field. Φ
 - λ and μ^2 are Higgs potential parameters



SM Lagrangian

Yukawa lagrangian

$$\mathcal{L}_{yukawa} = \Gamma_{mn}^u q_{m,L} \tilde{\phi} u_{n,R} + \Gamma_{mn}^d \bar{q}_{m,L} \phi d_{n,R} + \Gamma_{mn}^e \bar{l}_{m,L} \phi e_{n,R} + h.c \quad (2)$$

where $h.c$ is hermitian conjugate.

The matrices Γ_{mn} describe the so called Yukawa couplings between higgs doublet ϕ and the fermions.

Choosing

$$\Phi = -\frac{1}{2} \begin{pmatrix} 0 \\ v+h \end{pmatrix} \rightarrow \Phi = \frac{1}{2} \begin{pmatrix} 0 \\ v \end{pmatrix}$$

By using it on the first part of the lagrangian it is obtained

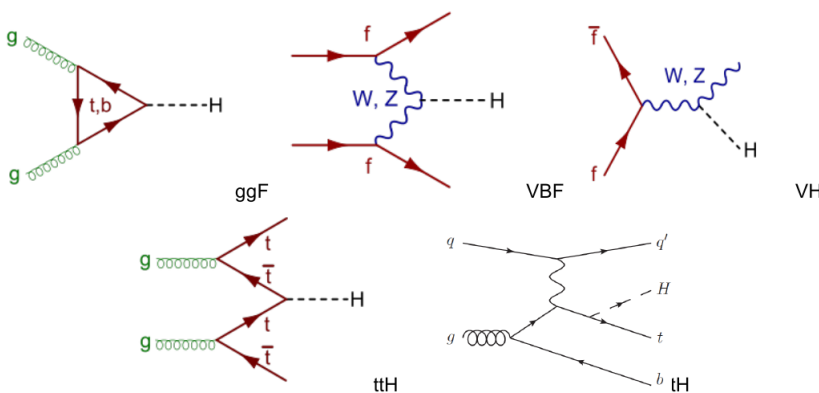
$$\frac{f_u v}{\sqrt{2}(\bar{u}_L u_R + \bar{u}_R u_L)}$$

from which the masses for the fermions in question can be read off:

$$m_{\pm} = \frac{f_u v}{\sqrt{2}}$$



Higgs production mechanisms



tH production mechanisms

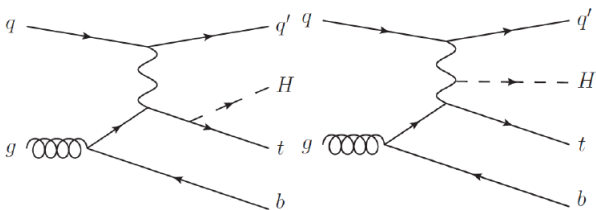


Figure: tH mechanism. Higgs radiated from a top quark (left). Higgs radiated from a W boson (right)

tH production mechanisms

- In a proton proton collision, the production cross section of the single top plus Higgs boson (tHq) process is driven by a destructive interference of two main diagrams (see Fig. 1.), where the Higgs couples to either the W boson or the top quark.
- A second process, where the Higgs and top quark are accompanied by a W boson (tHW) has similar behavior, albeit with a weaker interference pattern.
- However, in the presence of new physics, there may be relative opposite signs between the tH and WH couplings which lead to constructive interference and enhance the cross sections by an order of magnitude or more.

Cross section

- Classical definition: When two particles interact, cross section is the area transverse to their relative motion within which they must meet in order to scatter from each other.
- Quantum definition: Cross section describes the likelihood of two particles interacting under certain conditions[1]
- Experimentally

$$d\sigma = \frac{\text{number of particles scattered into solid angle } \Delta\Omega}{(\text{number of particles incident})(\text{scattering centers/area})} \quad (3)$$

- Cross sections are expressed in barns , where $1 \text{ barn} = 10^{-34} \text{ cm}^{-2}$

Cross section

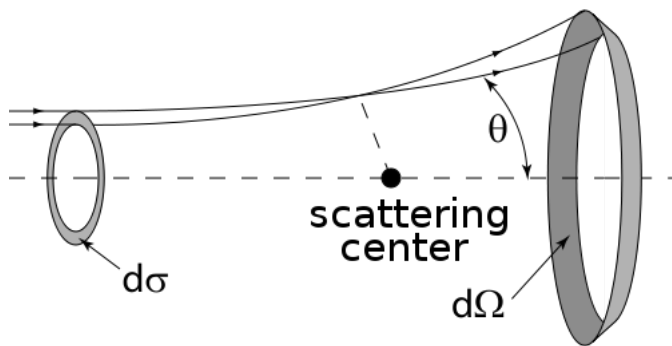


Figure: Drawing of an idealized scattering process showing the differential solid angle $\Delta\Omega$ and the scattering angle θ

Cross section

The reaction rate N_R is determined by the total cross section σ and the incident flux L .

L is called luminosity and it is measured in $\text{cm}^{-1}\text{s}^{-1}$.

$$N_R = \sigma L \quad (4)$$

Higgs production Cross section

Higgs boson production cross sections in pp collisions for $\sqrt{s} = 13\text{TeV}$ (in pico barn). Integrated luminosity of 35.9 fb^{-1} for Run 2¹

Production mechanism	σ (picobarns pb)	Number of events
ggF	48.93	1756587
VBF	3.78	135702
WH	1.35	48465
ZH	0.88	31592
t \bar{t} H	0.50	18255
tH (only)	0.015	560.39

¹ Data taken from The cern collaborarion "Higgs Physics the HL-LHC and HE-LHC" 2019,
CERN-LPCC-2018-04

Higgs production cross section

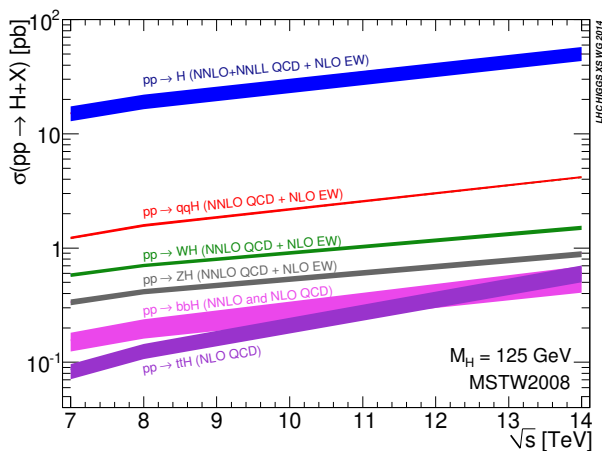


Figure: Higgs boson production cross sections as a function of the centre-of-mass-energies

Branching ratio

In particle physics, the branching ratio for a decay process is the ratio of the number of particles which decay via a specific decay mode with respect to the total number of particles which decay via all decay modes.

3

$$\text{BR} = \frac{\Gamma_i}{\sum_i \Gamma_i} \quad (5)$$

Where $\Gamma = \sum_i \Gamma_i$ is the total decay width (sum of all partial widths) of the particle and is related to lifetime of the particle: $\Gamma = 1/\tau$. Since the dimension of Γ is the inverse of time, in our system of natural units, it is measured in inverse seconds.⁰

⁰ Cleaves H.J. (2011) Branching Ratio. In: Gargaud M. et al. (eds) Encyclopedia of Astrobiology. Springer, Berlin, Heidelberg

Higgs Branching ratio

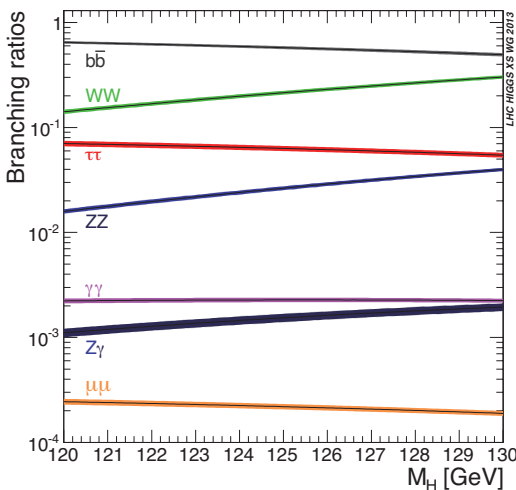


Figure: Standard Model Higgs boson decay branching ratios

Higgs Branching ratios per channel

SM Higgs boson branching ratios for $M_H = 125$ GeV

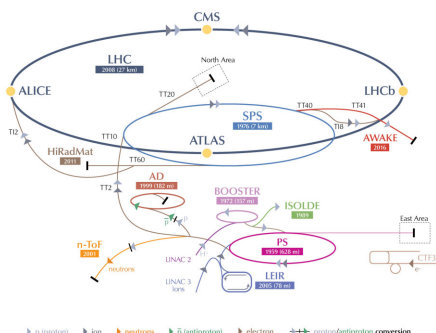
Higgs decay	Branching ratio (BR)
$H \rightarrow b\bar{b}$	50.82%
$H \rightarrow W^+ W^-$	21.5%
$H \rightarrow \tau^+ \tau^-$	6.27%
$H \rightarrow ZZ$	2.61%
$H \rightarrow \gamma\gamma$	0.227%
$H \rightarrow Z\gamma$	0.153%
$H \rightarrow \mu^+ \mu^-$	0.0217%

$\mu\mu$ same sign decay rate

Table of decay chains for tH. Expected number of final events assuming 560 produced tH events. l represents μ^\pm, e^\pm, τ^\pm

Decay chain	BR	Events
$tH \rightarrow W^+ b W^+ W^- \rightarrow \mu^+ \nu_\mu b \mu^+ \nu_\mu q \bar{q}'$	2.096×10^{-3}	1.173
$tH \rightarrow W^+ b W^+ W^- \rightarrow \mu^+ \nu_\mu b \mu^+ \nu_\mu l^- \bar{\nu}_l$	3.37×10^{-4}	0.899
$tH \rightarrow W^+ b \tau^+ \tau^- \rightarrow \mu^+ \nu_\mu b \mu^+ \nu_\mu \bar{\nu}_\tau l^- \bar{\nu}_l \nu_\tau$	3.637×10^{-4}	0.203
$tH \rightarrow W^+ b W^+ W^- \rightarrow \tau^+ \bar{\nu}_\tau b \mu^+ \nu_\mu q \bar{q} \rightarrow \mu^+ \nu_\mu \bar{\nu}_\tau \bar{\nu}_\tau b \mu^+ \nu_\mu q \bar{q}$	1.890×10^{-4}	0.105
$tH \rightarrow W^+ b \tau^+ \tau^- \rightarrow \mu^+ \nu_\mu b \nu_\tau \mu^+ \nu_\mu \bar{\nu}_\tau q \bar{q}$	1.681×10^{-4}	0.094
$tH \rightarrow W^+ b W^+ W^- \rightarrow \tau^+ \bar{\nu}_\tau b \mu^+ \nu_\mu l^- \bar{\nu}_l \rightarrow \mu^+ \nu_\mu \bar{\nu}_\tau \bar{\nu}_\tau b \mu^+ \nu_\mu l^- \bar{\nu}_l$	3.045×10^{-5}	0.017
$tH \rightarrow W^+ b ZZ \rightarrow q \bar{q} b ZZ \rightarrow q \bar{q} b \mu^+ \mu^- \mu^+ \mu^-$	1.966×10^{-5}	0.011
$tH \rightarrow W^+ b \tau^+ \tau^- \rightarrow \tau^+ \bar{\nu}_\tau b \mu^+ \nu_\mu \bar{\nu}_\tau q \bar{q}' \nu_\tau \rightarrow \mu^+ \nu_\mu \bar{\nu}_\tau \bar{\nu}_\tau b \mu^+ \nu_\mu \bar{\nu}_\tau q \bar{q}' \nu_\tau$	1.549×10^{-5}	0.008

CERN's Accelerator Complex



LHC Large Hadron Collider SPS Super Proton Synchrotron PS Proton Synchrotron

AD Antiproton Decelerator CTF3 Clic Test Facility AWAKE Advanced WAKEfield Experiment ISOLDE Isotope Separator OnLine Dvice

LEIR Low Energy Ion Ring LINAC LINear ACcelerator n-ToF Neutrons Time Of Flight HiRadMat High-Radiation to Materials

©CERN 2011

LHC parameters

Quantity	Number
Circumference	26 659 m
Dipole operating temperature	1.9 K (-271.3°C)
Number of magnets	9593
Number of main dipoles	1232
Number of main quadrupoles	392
Number of RF cavities	8 per beam
Nominal energy, protons	6.5 TeV
Nominal energy, ions	2.56 TeV/u (energy per nucleon)
Nominal energy, protons collisions	13 TeV
No. of bunches per proton beam	2808
No. of protons per bunch (at start)	1.2×10^{11}
Number of turns per second	11245
Number of collisions per second	1 billion

Table. LHC characteristics for run 2.

Accelerator operation energies

Accelerator	Energy
Linac 2	50 MeV
PS Booster	1.4 GeV
Proton Scyncroton (PS)	25 GeV
SPS	450 GeV
LHC	6.5 TeV

CMS detector

CMS DETECTOR

Total weight : 14,000 tonnes

Overall diameter : 15.0 m

Overall length : 28.7 m

Magnetic field : 3.8 T

STEEL RETURN YOKE
12,500 tonnes

SILICON TRACKERS
Pixel (100x150 μ m) ~16m² ~66M channels
Microstrips (80x180 μ m) ~200m² ~9.6M channels

SUPERCONDUCTING SOLENOID
Niobium titanium coil carrying ~18,000A

MUON CHAMBERS
Barrel: 250 Drift Tube, 480 Resistive Plate Chambers
Endcaps: 468 Cathode Strip, 432 Resistive Plate Chambers

PRESHOWER
Silicon strips ~16m² ~137,000 channels

FORWARD CALORIMETER
Steel + Quartz fibres ~2,000 Channels

CRYSTAL
ELECTROMAGNETIC
CALORIMETER (ECAL)
~76,000 scintillating PbWO₄ crystals

HADRON CALORIMETER (HCAL)
Brass + Plastic scintillators ~7,000 channels

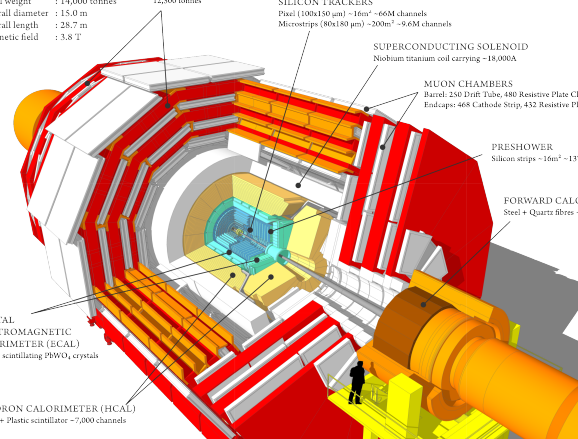


Figure: Compact muon solenoid

CMS integrated luminosity

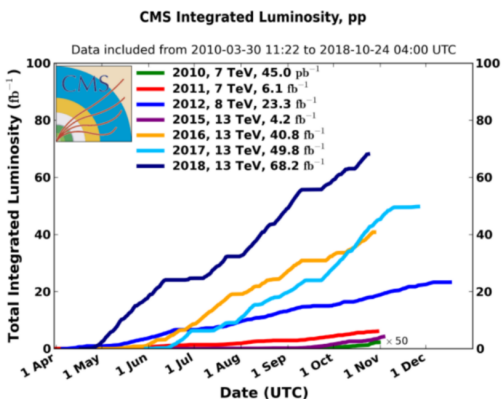
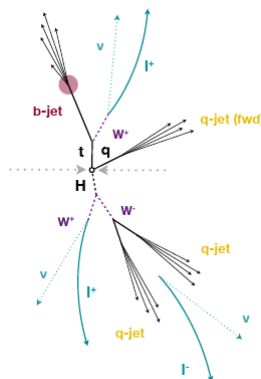


Figure: Integrated luminosity for CMS experiment

Topology of events tH

The characteristics of the signal th:

- $t \rightarrow W^+ b \rightarrow l^+ \nu_\mu b$
 - $H \rightarrow W^+ W^-$
 - $W \rightarrow l^\pm \nu$, where l can be μ^\pm, e^\pm, τ^\pm
 - $W \rightarrow q\bar{q}$
 - W bosons decay leptonically resulting in a signature of two same-sign leptons
 - a light-flavor quark
 - b quark jet [2]



Event selection

The main analysis strategy is to obtain a selection of events compatible with certain characteristics of the signal at pre-selection level.

It is required:

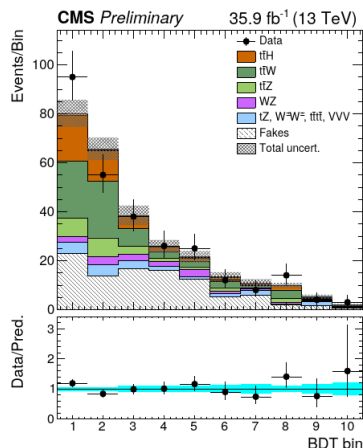
- The events are selected those that contain two leptons (l^+l^-) with the same sign.
- Transverse moment $p_t > 25$ and 15 GeV, for the muons.
- A forward jet with $p_t > 40$ GeV, $| \eta | > 2.4$
- One or more b-jets with ($| \eta | < 2.4$)[1]

Previous results

- Direct searches for tHq production using all relevant Higgs decay modes have previously been carried out by CMS in the 8 TeV dataset in pp collisions[4]
- On 2015, in pp collisions with $\sqrt{s}=13$ TeV data set using the $H \rightarrow b\bar{b}$ channel, corresponding to an integrated luminosity of 35.9 fb^{-1} [6]
- In 2016, for $\sqrt{s}= 13$ TeV dataset, a search for $t\bar{t}H$ production in multilepton final states recently produced first evidence for associated production of top quarks and Higgs bosons[2]

Previous results for $t\bar{t}H$ production

Process	$\mu\mu$
$t\bar{t}W^\pm$	68.03 ± 0.61
$t\bar{t}Z/t\bar{t}\gamma$	25.89 ± 1.12
WZ	15.07 ± 1.19
ZZ	1.16 ± 0.29
$W^\pm W^\pm qq$	3.96 ± 0.52
$W^\pm W^\pm$ (DPS)	2.48 ± 0.42
VVV	2.99 ± 0.34
ttt	2.32 ± 0.45
tZq	5.77 ± 2.24
tZW	2.13 ± 0.13
γ conversions	—
Non-prompt	80.94 ± 2.02
Charge flips	—
Total Background	210.74 ± 3.61
$t\bar{t}H$	24.18 ± 0.48
tHq (SM)	1.43 ± 0.04
tHW (SM)	0.71 ± 0.03
Total SM	237.06 ± 3.64
$t\bar{t}Hq$ ($\kappa_V = 1 = -\kappa_t$)	18.48 ± 0.22
$t\bar{t}HW$ ($\kappa_V = 1 = -\kappa_t$)	7.72 ± 0.17
Data	280



Post-fit categorized BDT classifier outputs as used in the maximum likelihood fit for the $\mu\mu$ channel for 35.9 fb^{-1} . In the box below each distribution, the ratio of the observed and predicted event yields is shown. [2]

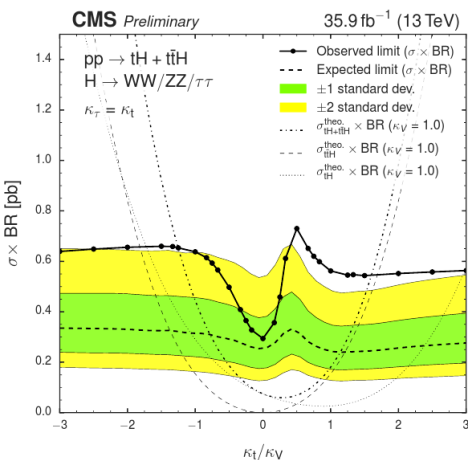


Figure: Observed and expected 95% C.L. upper limit on the $\text{tH} + \bar{\text{t}}\text{H}$ cross section times $\text{H} \rightarrow \text{WW} + \tau\tau + \text{ZZ}$ branching fraction for different 20 values of the coupling ratio κ_t/κ_V . The expected limit is derived from a background-only MC dataset.

Main backgrounds

In the leptonic channels, the main backgrounds are expected to arise from the production of top quarks

- In the dominant $t\bar{t}$ mode, where same-sign dilepton signatures can occur when a non-prompt lepton from heavy-flavor decay passes the signal selection, or in associated production with a W/Z or Higgs boson.
- Processes with single top quarks also contribute, mostly in the associated production with a Z boson (tZ) or when produced with both a W and a Z boson (WZ)

Main backgrounds

- $t\bar{t}W^\pm$ and $t\bar{t}Z$ ($t\bar{t}V$): Backgrounds are estimated directly from simulated events
- WZ: Diboson production with leptonic Z decays and additional jet radiation in the final state can lead to signatures very similar to that of the signal. Due to the larger cross section, the main contribution arises from WZ production.
- $t\bar{t}H$: tHq production which decays to same sign dileptons.
- Rare SM ($tZ, VVV, WW, tttt$): Due to small event yields, all these processes are grouped as one.
- Non prompt leptons b quark decays and spurious lepton signatures from hadronic jets.

Main backgrounds

Background	$\sigma[\text{pb}]$	Decay process
t \bar{t} H	0.2151	$t\bar{t}H \rightarrow W^+b W^+b WW \rightarrow \mu^+\nu_\mu b\mu^-\bar{\nu}_\mu \bar{b} \mu^+\mu^-\mu^+\mu^-$
t \bar{t} W and	0.2043	$t\bar{t}W \rightarrow W^+b W^+b\mu^+\mu^- \rightarrow \mu\nu_\mu b\mu\nu_\mu b\mu^+\mu^-$
t \bar{t} Z	0.2529	$t\bar{t}Z \rightarrow W^+b W^-b\mu^+\mu^- \rightarrow \mu^+\nu_\mu b \mu^-\bar{\nu}_\mu \bar{b}$
W $^+W^-$	1.64	$WW \rightarrow \mu^+\mu^-\mu^-\mu^+$
tZq	0.0758	$tZq \rightarrow W^+b\mu^+\mu^- q \rightarrow \mu^+\nu_\mu b \mu^+\mu^- q$
tttt	0.0091	$tttt \rightarrow W^+bW^+bW^+bW^+b \rightarrow \mu^+\nu_\mu b\mu^+\nu_\mu b q\bar{q}b q\bar{q}b$
WZZ	0.1651	$WZZ \rightarrow \mu^+\mu^-\mu^+\mu^-l^+l^-$
ZZZ	0.0139	$ZZZ \rightarrow \mu^+\mu^-\mu^+\mu^-l^+l^-$
WZZ	0.0556	$WZZ \rightarrow \mu^+\mu^-\mu^+\mu^-l^+l^-$
WZ	4.42965	$WZ \rightarrow \mu^+\mu^-\mu^+\mu^-$
ZZ	1.256	$ZZ \rightarrow \mu^+\mu^-\mu^+\mu^-$

- Rare SM: tttt, WWW, WWZ, WZZ, WW, tZq
- WZ: WZ, ZZ

Boosted decision tree (BDT)

- A decision tree takes a set of input features and splits input data recursively based on those features. Boosting is a method of combining many weak learners (trees) into a strong classifier. The features can be a mix of categorical and continuous data.
 - The BDT training is performed using several event variables for signal and background.
 - BDT training uses MC samples for $t\bar{t}W^\pm$ and $t\bar{t}Z$ ($t\bar{t}V$), because $t\bar{t}V$ is one of the biggest backgrounds

BDT Variables

- Trailing lepton p_t
- Total charge of tight leptons
- $\min \Delta R$ (lepton pairs)
- $\Delta\phi$ between highest p_t lepton pair
- Number of jets with $|\eta| < 2.4$
- Number of non b-tagged jets with $|\eta| > 1.0$
- Maximum $|\eta|$ for jets
- $\Delta\eta$ (most forward light jet, closest lepton)
- $\Delta\eta$ (most forward light jet, hardest loosely b-tagged jet)
- $\Delta\eta$ (most forward light jet, 2nd hardest loosely b-tagged jet)

Sources of uncertainty on event yields

- Luminosity measurement: 2.6%.
- Data/MC scale factors for lepton selection (ID, iso) and trigger efficiencies 5% per lepton.
- Choice of PDF set:
 - 3.7% for tHq
 - 4% for tHW, $t\bar{t}W$, $t\bar{t}Z$, $t\bar{t}H$
 - Scale uncertainties: 12%, 4% for $t\bar{t}W$, 10% for $t\bar{t}Z$, +5.8/-9.2% for $t\bar{t}H$.
- Background: WZ, ZZ sample modelling and statistics: 50%.
- Rare SM (tZ, tri-bosons, WWqq, tt) : 50%
- Fake rate estimation: The predicted event yield has a normalization uncertainty of 30-50% [7]

Uncertainty values

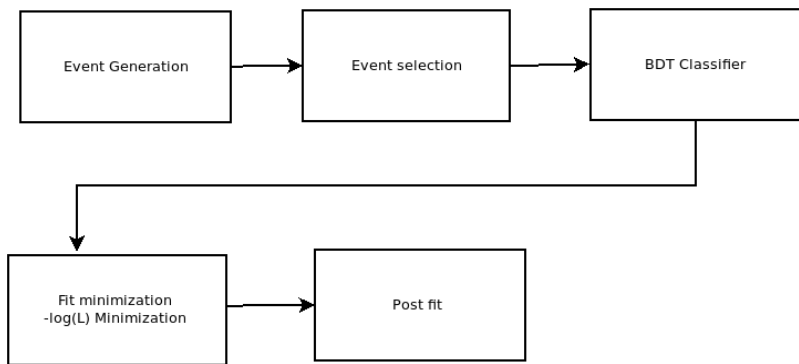
Common uncertainties for MC :

- Muon identificacion 6%
 - Dimuon Trigger 1%

Background	Sources of systematic uncertainty	Total Systematic Uncertainty
$t\bar{t}H$	<ul style="list-style-type: none"> PDF 4% QCD scale 5.8% Higgs BR 1% 	9.36%
$t\bar{t}Z$	<ul style="list-style-type: none"> PDF 4% QCD scale 10% 	12.36 %
$t\bar{t}W$	<ul style="list-style-type: none"> PDF 4% QCD scale 12% 	14.03 %

Background	Sources of systematic uncertainty	Total Systematic Uncertainty
Rares SM	<ul style="list-style-type: none">Rare SM 50%	50.36 %
WZ	<ul style="list-style-type: none">Sample modelling and statistics 50%	50.36%
Non prompt leptons	<ul style="list-style-type: none">Fake rate estimation 50%Closure 7%	50.48%

Fitting



Likelihood model

The likelihood function is the product of Poisson probabilities for all bins

$$L(\mu, \theta) = \prod_{j=1}^N \frac{(\mu s_j + b_j)^{n_j}}{n_j!} e^{-(\mu s_j + b_j)} \quad (6)$$

- N=number of bins
- μ =parameter of signal
- s=signal
- b=background
- n=number of events

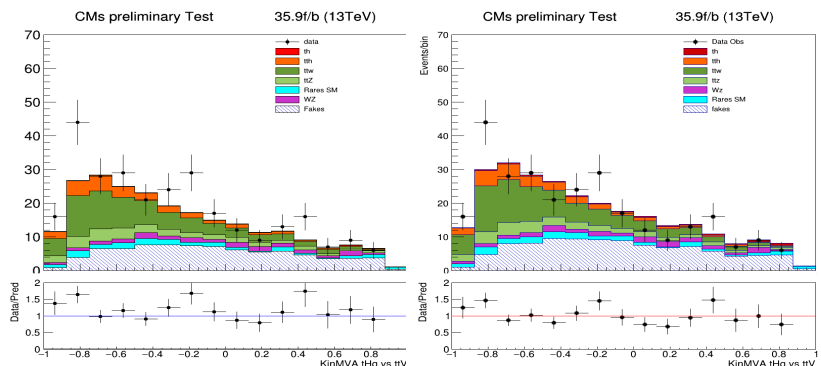
Results

Table: Prefit and postfit table for each yield.

Process	Number of events prefit	Number of events Postfit
tH	2.13 ± 0.21	5.36 ± 27.40
t <bar>t>H</bar>	24.18 ± 2.26	24.81 ± 2.24
t <bar>t>W</bar>	68.03 ± 9.54	77.01 ± 8.76
t <bar>t>Z</bar>	25.89 ± 3.20	26.74 ± 3.18
Rares SM	17.17 ± 8.64	18.77 ± 8.66
WZ	16.23 ± 8.17	17.41 ± 8.04
fakes	80.94 ± 40.86	100.15 ± 29.30

Prefit uncertainty is statistical only. Postfit uncertainty is statistical + systematic.

Results



Pre-fit signal and background yields the box below each distribution, the and predicted event yields is shown

Post-fit signal and background yields for $t\bar{t}H$ process. In the box below each distribution, the ratio of the observed and predicted event yields is shown

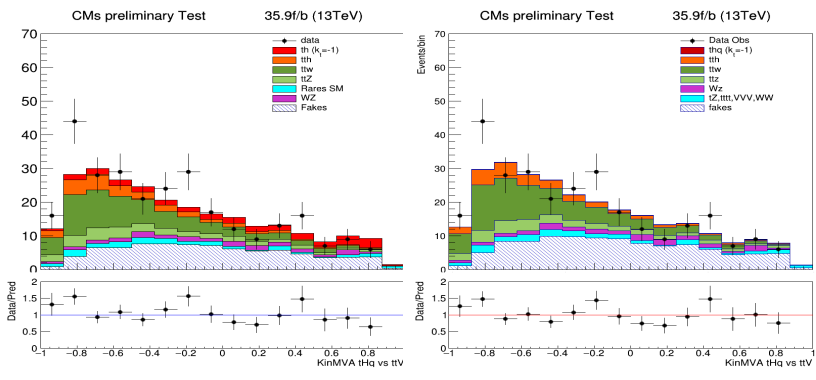
Results

Table: Prefit and postfit table for each yield. $k_t = -1$.

Process	Number of events prefit	Number of events Postfit
tH	26.2 ± 2.60	1.83 ± 26.63
t <bar>t</bar>	24.18 ± 2.26	24.82 ± 2.27
t <bar>t</bar>	68.03 ± 9.54	77.07 ± 8.99
t <bar>t</bar>	25.89 ± 3.20	26.76 ± 3.18
Rares SM	17.17 ± 8.64	18.90 ± 8.37
WZ	16.23 ± 8.17	17.54 ± 8.15
fakes	80.94 ± 40.86	102.97 ± 29.51

Prefit uncertainty is statistical only. Postfit uncertainty is statistical + systematic.

Results



Pre-fit signal and background yields for tH process for $k_t = -1$.

In the box below each distribution, the ratio of the observed and predicted event yields is shown

Post-fit signal and background yields for tH process for $k_t = -1$.

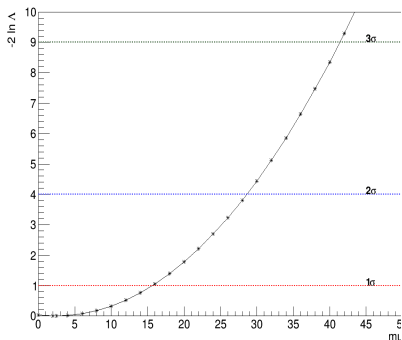
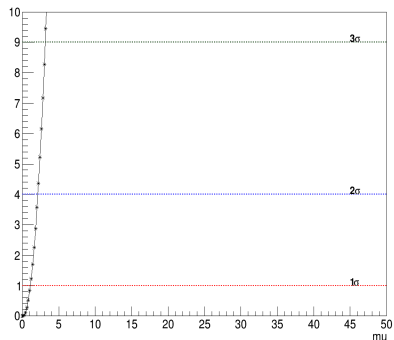
In the box below each distribution, the ratio of the observed and predicted event yields is shown

Test statistic q_μ for upper limits

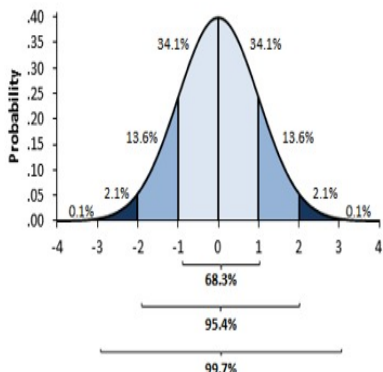
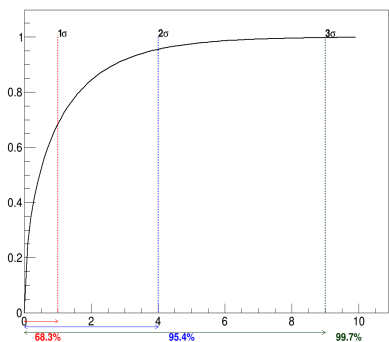
For purposes of establishing an upper limit on the strength parameter μ , we consider two closely related test statistics. First, we may define

$$q_\mu = \begin{cases} -2 \ln \lambda(\mu) & \hat{\mu} \leq \mu \\ 0 & \hat{\mu} < 0 \end{cases}$$

The reason for setting $q_\mu = 0$ for $\hat{\mu} > \mu$ is that when setting an upper limit, one would not regard data with $\hat{\mu} > \mu$ as representing less compatibility with μ than the data obtained, and therefore this is not taken as part of the rejection region of the test. From the definition of the test statistic one sees that higher values of q_μ represent greater incompatibility between the data and the hypothesized value of μ .

Likelihood scan for $k_t=1$ (SM)Likelihood scan for $k_t=-1$

Test statistic q_μ for upper limits

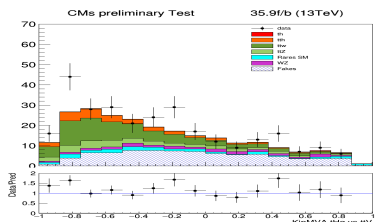


Test statistic q_μ for upper limits

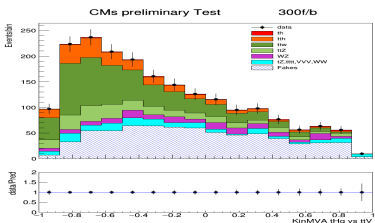
Table for estimation of μ for fitting and upper limit with luminosity of 35.9 fb^{-1}

Model	μ	μ upper limit
SM ($K_t = 1$)	$2.4975\text{e+00} \pm 1.29\text{e+01}$	28.047
$K_t = -1$	$6.9361\text{e-02} \pm 1.02\text{e+00}$	1.97

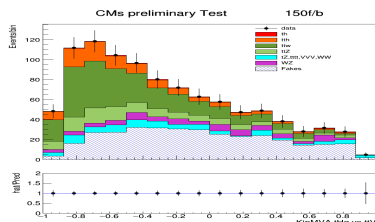
Extrapolation of luminosity



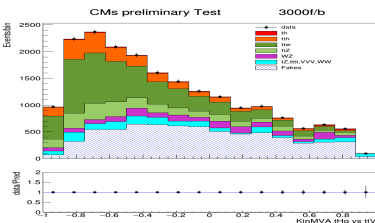
35.9 fb^{-1}



300 fb⁻¹

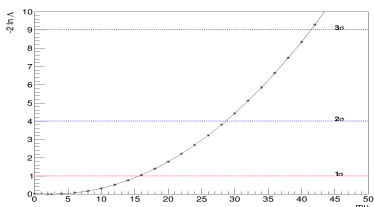


150 fb^{-1}

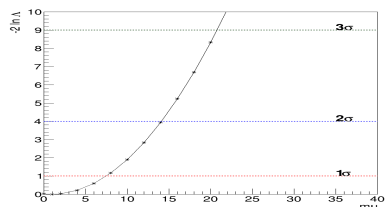


$\sim 3000 \text{ fb}^{-1}$

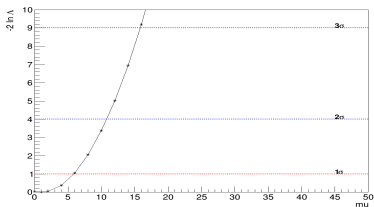
Likelihood scan



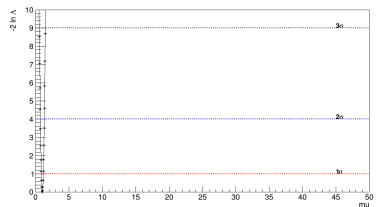
35.9 fb^{-1}



150 fb^{-1}

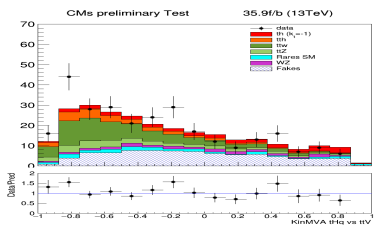


300 fb^{-1}

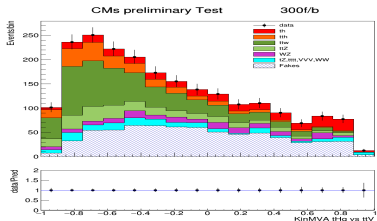


3000 fb^{-1}

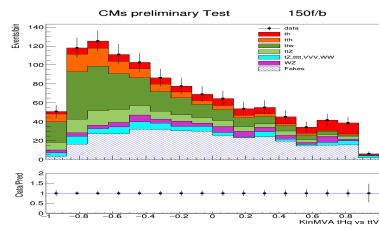
Extrapolation of luminosity for $k_t = -1$



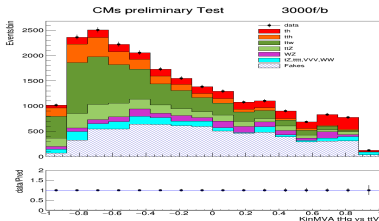
35.9 fb^{-1}



300 fb⁻¹

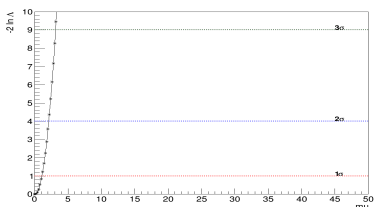


150 fb^{-1}

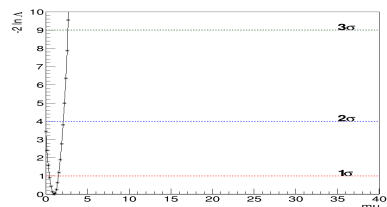


$\sim 3000 \text{ fb}^{-1}$

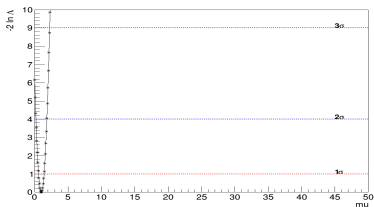
Likelihood scan for $k_t = 1$



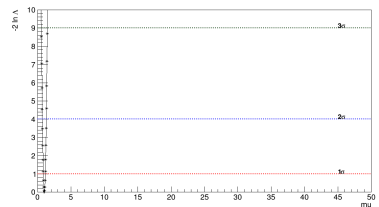
35.9 fb^{-1}



150 fb^{-1}



300 fb⁻¹



$\sim 3000 \text{ fb}^{-1}$

Estimation of μ

Luminosity (fb^{-1})	μ	μ for $k_t = -1$	μ upper limit	μ upper limit for $k_t = 1$
35.9	$2.4975\text{e+00} \pm 1.29\text{e+01}$	$6.9361\text{e-02} \pm 1.02\text{e+00}$	28.047	1.97
150	$1.0000\text{e+00} \pm 6.44\text{e+00}$	$1.0000\text{e+00} \pm 5.44\text{e-01}$	12.619	0.915
300	$1.0000\text{e+00} \pm 4.83\text{e+00}$	$1.0000\text{e+00} \pm 4.07\text{e-01}$	9.427	0.649
3000	$1.0000\text{e+00} \pm 1.54\text{e+00}$	$1.0000\text{e+00} \pm 1.51\text{e-01}$	3.442	0.25

References

-  Gross F. *Relativistic quantum mechanics and field theory* 1994 Wiley
-  The CMS collaboration, *Search for production of a Higgs boson and a single top quark in multilepton final states in proton collisions at 13 TeV*, CMS-PAS-HIG-17- 005
-  Verkerke W *Dealing with systematic uncertainties* 2014. From https://indico.cern.ch/event/287744/contributions/1641261/attachments/535763/738679/Verkerke_Statistics_3.pdf

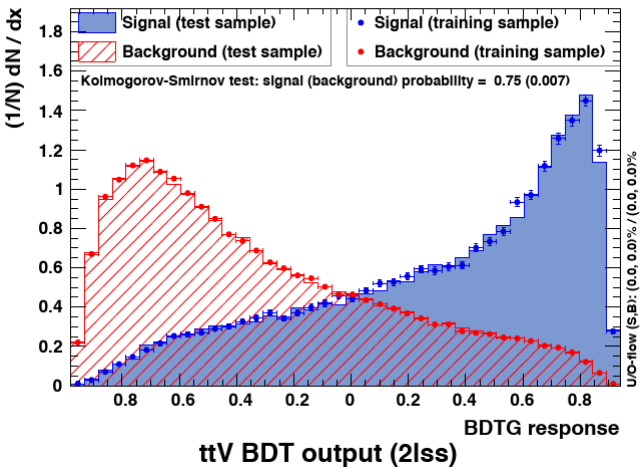
- ATLAS and CMS Collaborations, *Combined measurement of the Higgs boson mass in pp collisions at $\sqrt{s}=7$ and 8 TeV with the ATLAS and CMS experiments*, Phys. Rev. Lett. 114 (2015) doi:10.1103/PhysRevLett.114.191803, arXiv:1503.07589
 - Cowan G. , Cranmer K., Gross E. , Vitells O. *Asymptotic formulae for likelihood-based tests of new physics* 2013 , arXiv:1007.1727
 - CMS Collaboration, *Search for the $tH(H \rightarrow b\bar{b})$ process in the pp collisions at $\sqrt{s}=13$ TeV and study of Higgs boson couplings* 2018,CMS PAS HIG-17-016
 - CMS collaboration *Search for tHq production in multilepton final states at 13 TeV* ,2017,CMS AN-16-378

Back up

BDT parameters

- Gradient boosted (BDTG)
- No. of trees = 800
- No. of cuts = 50
- Maximum depth = 3
- Found to be most discriminating, minimal overtraining.

TMVA overtraining check for classifier: BDTG



List of histograms used in the analysis

Data taken from the file `plots-thq-2lss-kinMVA.root` 2016
CERN

- `thqMVA_ttv_2lss_40_tZq`
- `thqMVA_ttv_2lss_40_ttz`
- `thqMVA_ttv_2lss_40_VVV`
- `thqMVA_ttv_2lss_40_ttw`
- `thqMVA_ttv_2lss_40_data_fakes`
- `thqMVA_ttv_2lss_40_tth`
- `thqMVA_ttv_2lss_40_tHW_hww`
- `thqMVA_ttv_2lss_40_WWss`
- `thqMVA_ttv_2lss_40_tttt`
- `thqMVA_ttv_2lss_40_WZ`
- `thqMVA_ttv_2lss_40_tHq_hww`

Backgrounds and signal histograms

tHq: Signal (tH)

- thqMVA_ttv_2lss_40_tHq_hww
- thqMVA_ttv_2lss_40_tHW_hww

Backgrounds

t \bar{t} W

- thqMVA_ttv_2lss_40_ttW

t \bar{t} Z

- thqMVA_ttv_2lss_40_ttZ

WZ

- thqMVA_ttv_2lss_40_WZ

Backgrounds and signal histograms

Backgrounds

tZ, VVV,tttt,WW:

- thqMVA_ttv_2lss_40_tZq
- thqMVA_ttv_2lss_40_WWss
- thqMVA_ttv_2lss_40_VVV
- thqMVA_ttv_2lss_40_tttt

t \bar{t} H

- thqMVA_ttv_2lss_40_ttH

Non prompt leptons (fakes)

- thqMVA_ttv_2lss_40_data_fakes

Closure: hay jets en los eventos de $t\bar{t}$ (gluon-gluon $\rightarrow t\bar{t} + \text{gluon}$) que se pasan como muones. jet \rightarrow muon = fake

Fakes: proceso de QCD que genera muchos jets (por ejemplo gluon-gluon \rightarrow gluons, quarks) : jet \rightarrow muons fakes are estimated data

¹

¹Due to existence of many uncertainties, it is necessary to sum all the uncertainties. When there is no Correlation, the uncertainties must be summed as the square root of the squares of each uncertainty

Sources of systematic uncertainty

Detector-simulation related uncertainty

- Calibrations (electron, jet energy scale)
- Efficiencies (particle ID, reconstruction)
- Resolutions (jet energy, muon momentum)

Theoretical uncertainties

- Factorization/Normalization scale of MC generators
- Choice of MC generator (ME and/or PS, e.g. Herwig vs Pythia)

Monte Carlo Statistical uncertainties

- Statistical uncertainty of simulated samples[2]

Observed events

- After applying the event pre-selection on the dataset, 280 events are observed in the same-sign $\mu\mu$ channel
- The events are then sorted into ten categories depending on the output of the two BDT classifiers according to an optimized binning strategy, resulting in a one-dimensional histogram with ten bins.
- In each point, the tH and $t\bar{t}H$ production cross sections and the Higgs decay branching ratios are modified with the Higgs-top (κ_t) and Higgs-vector boson (κ_v) coupling strength.
- The Higgs-tau coupling strength modifier (κ_τ) is assumed to be equal to κ_t .
- All other parameters are assumed to be at the values predicted by the standard model[1].

α values for post fit

Floating Parameter	FinalValue	+/- Error
Lumi	1.0082e+00	+/- 2.42e-02
alpha_sample_tth_sys	1.9100e-01	+/- 9.94e-01
alpha_sample_ttw_sys	8.7537e-01	+/- 9.18e-01
alpha_sample_ttz_sys	2.0012e-01	+/- 9.95e-01
alpha_sample_tz_sys	1.6749e-01	+/- 1.00e+00
alpha_sample_wz_sys	1.2732e-01	+/- 9.84e-01
alpha_sample_fakes_sys	4.5030e-01	+/- 7.17e-01
mu	2.4975e+00	+/- 1.29e+01

α values for post fit thq $k_t = -1$

Floating Parameter	FinalValue	+/- Error
Lumi	1.0085e+00	+/- 2.40e-02
alpha_sample_tth_sys	1.9290e-01	+/- 1.00e+00
alpha_sample_ttw_sys	8.7911e-01	+/- 9.42e-01
alpha_sample_ttz_sys	2.0370e-01	+/- 9.94e-01
alpha_sample_tz_sys	1.8269e-01	+/- 9.69e-01
alpha_sample_wz_sys	1.4244e-01	+/- 9.99e-01
alpha_sample_fakes_sys	1.4243e-01	+/- 9.98e-01
mu	6.9361e-02	+/- 1.02e+00

Results

Likelihood scan

- Likelihood function (often simply the likelihood) is a function of the parameters of a statistical model, given specific observed data.
- Likelihood functions play a key role in frequentist inference, especially methods of estimating a parameter from a set of statistics.
- In informal contexts, "likelihood" is often used as a synonym for probability.

Results

Likelihood scan

To test a hypothesized value of μ we consider the profile likelihood ratio

$$\lambda(\mu) = \frac{L(\mu, \hat{\theta})}{L(\hat{\mu}, \hat{\theta})} \quad (7)$$

- Here $\hat{\theta}$ in the numerator denotes the value of θ that maximizes L for the specified μ , it is the conditional maximum-likelihood (ML) estimator of $\hat{\theta}$ (and thus is a function of μ). The denominator is the maximized (unconditional) likelihood function, i.e., $\hat{\mu}$ and $\hat{\theta}$ are their ML estimators[3].
- The presence of the nuisance parameters broadens the profile likelihood as a function of μ relative to what one would have if their values were fixed. This reflects the loss of information about μ due to the systematic uncertainties[3][5].

Statistical test

It is convenient to use the statistic

$$t_\mu = -2 \ln \lambda(\mu) \quad (8)$$

as the basis of a statistical test. Higher values of t_μ thus correspond to increasing incompatibility between the data and μ . We may define a test of a hypothesized value of μ by using the statistic t_μ directly as measure of discrepancy between the data and the hypothesis, with higher values of t_μ correspond to increasing disagreement[5]

Statistical test

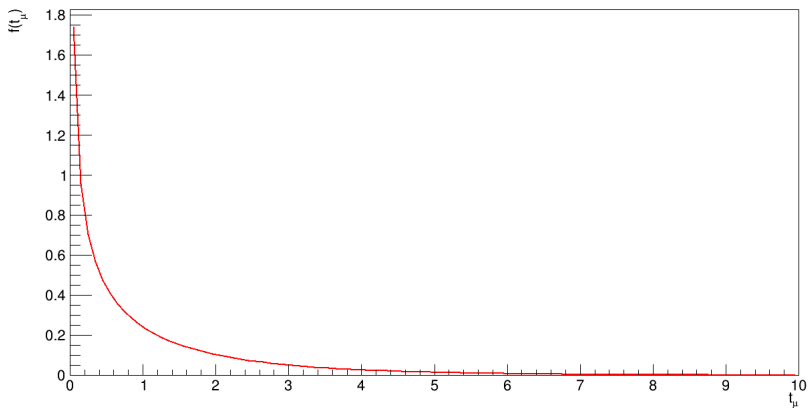


Figure: Statistic test plot $f(t_\mu)$ vs t_μ with $t_\mu = -2 \ln \lambda(\mu)$

P value

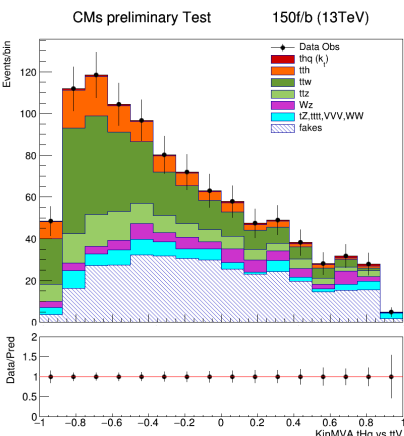
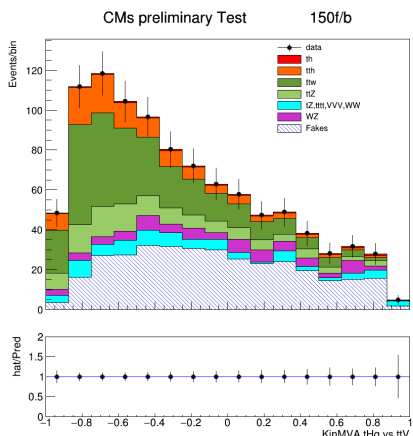
To quantify the level of disagreement we compute the P-value

$$P_\mu = \int_{t_\mu}^{\infty} f(t_\mu | \mu) dt_\mu \quad (9)$$

where t_μ is the value of the statistic t_μ observed from the data and $f(t_\mu | \mu)$ denotes the PDF (Probability density function) of t_μ under the assumption of the signal strength μ [5]

Luminosity scale

150 fb



Prefit

Post fit

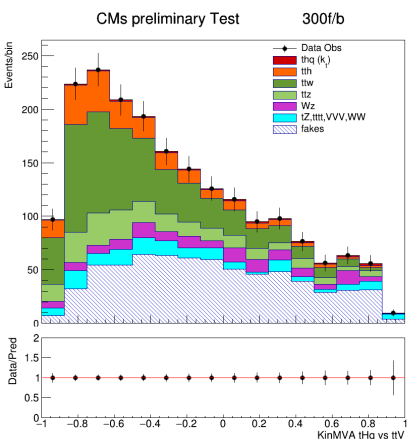
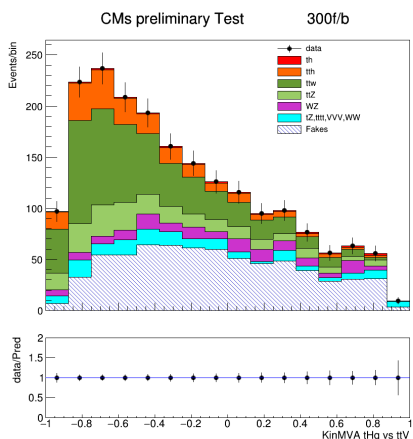
Luminosity scale

150 fb

event	N prefit	N Postfit
tH	8.89972 ± 0.885511	8.89972 ± 57.2784
ttH	101.031 ± 9.45	101.031 ± 9.27757
ttW	284.248 ± 39.8961	284.248 ± 31.3604
ttZ	108.175 ± 13.3806	108.175 ± 13.1161
tZ	71.7409 ± 34.1567	71.7409 ± 31.8423
WZ	$67.8134 \pm$	67.8134 ± 31.8861
fakes	338.189 ± 170.744	338.189 ± 84.302

Luminosity scale

300 fb



Prefit

post fit

Luminosity scale

300 fb

Table of yields for background and signal

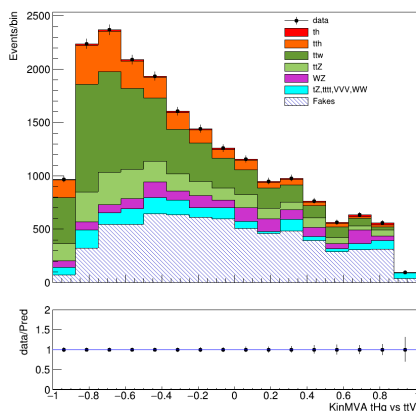
tH	17.7994 \pm	17.7994 \pm 85.9204
ttH	202.061 \pm 18.9162	202.061 \pm 18.4728
ttW	568.496 \pm 79.7922	568.496 \pm 56.3133
ttZ	216.351 \pm 26.7611	216.351 \pm 26.099
tZ	143.482 \pm 72.2699	143.482 \pm 58.5044
WZ	135.627 \pm 68.3133	135.627 \pm 60.7892
fakes	676.379 \pm 341.488	676.379 \pm 133.725

Luminosity scale

3000 fb

CMs preliminary Test

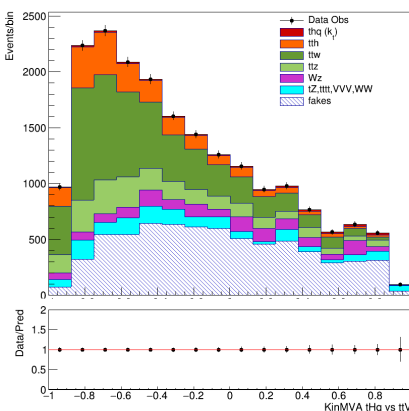
3000f/b



Prefit

CMs preliminary Test

3000f/b



Post fit

Luminosity scale

3000 fb

Table of yields for background and signal

event	N prefit	N Postfit
tH	5076.72 \pm 505.128	5076.72 \pm 643.706
ttH	2020.61 \pm 189.162	2020.61 \pm 183.997
ttW	5684.96 \pm 797.922	5684.96 \pm 561.487
ttZ	2163.51 \pm 267.611	2163.51 \pm 256.289
tZ	1434.82 \pm 722.699	1434.82 \pm 303.361
WZ	1356.27 \pm 683.133	1356.27 \pm 383.271
fakes	6763.79 \pm 3414.88	6763.79 \pm 591.597